Elongated Aggregates Formed by Cationic Gemini Surfactants

Reiko Oda,*,[†,‡] Ivan Huc,[§] Jean-Claude Homo,[‖] Benoit Heinrich,[⊥]
Marc Schmutz,[‖] and Sauveur Candau[†]

*Laboratoire de Dynamique des Fluides Complexes, 3 Rue de l'Université,
67000 Strasbourg, France, Laboratoire de Chimie Supramoléculaire, 4 Rue Blaise Pascal,
67000 Strasbourg, France, Institut de Physique et Chimie des Matériaux de Strasbourg,
23 Rue de Loess, 67000 Strasbourg, France, and Institut de Génétique et de Biologie
Moléculaire et Cellulaire, INSERM/CNRS/ULP, BP 163 67404, Illkirch Cedex, France*

The phase behavior of aqueous solutions of several dissymmetric gemini surfactants (with two hydrophobic chains of different lengths) was studied. From rheological and X-ray scattering studies as well as from freeze fracture imaging, some general patterns of the phase behavior were observed which are remarkably different from those observed for monomeric surfactants. The sequence of phases observed with increasing surfactant concentration was an isotropic wormlike micellar phase, multilayered structures which are first isotropic and then organized with orientational ordering, and an inverted hexagonal phase. The multilayered phase showed a scattering peak corresponding to a periodicity of 40 Å indicating the presence of stacks of bilayers without a water layer in between. For some of the samples, cryo-TEM showed that wormlike micelles (WLM) evolve into a ribbonlike structure (elongated bilayer). Upon further increase in concentration, the ribbons transform into multilayered structures with a well-defined width.

Introduction

For several decades, the relationship between the chemical structure of a surfactant and the morphology and physical properties of its aggregates in aqueous solutions has been the subject of intense experimental and theoretical work. A number of models have been proposed that take into account the effect of temperature, concentration, salt, or cosurfactants.[1] In many cases, these models permit a reasonably accurate prediction of the morphology and properties of surfactant assemblies. This applies especially when the surfactants possess a conventional structure with a single polar headgroup and one or two hydrophobic chains. In recent years, interest has grown for amphiphilic molecules with less usual structures from which new aggregates and physical properties may be expected. Among such new amphiphiles are the so-called dimeric or gemini surfactants.[2] These molecules are made of two (or more) conventional surfactant units connected by a spacer. The spacer can be long or short[3] and flexible or rigid.[4] It imposes a separation between the headgroups that may be shorter or longer than the average distance between the corresponding monomeric surfactants, thus modifying the mobility and the packing of the surfactants within the aggregate. A number of gemini surfactants have been described featuring cationic, anionic, neutral, nonchiral, or chiral headgroups.[5]

Bis(quaternary ammonium) surfactants having the structure C_sH_{2s}-α,ω-$(Me_2N^+C_mH_{2m+1}Br^-)_2$ are referred to as m–s–m. They appear in the literature as early as 1974[6] but have only recently been the object of a renewed interest. As most other gemini surfactants, they show very low critical micellar concentrations compared to those of the corresponding monomeric ammoniums.[2b] Both the roles of the spacer chain length[3] and the counterion[7] have been investigated. As shown by Zana et al.,[3] when $s \leq 5$, the positive charges within the gemini are held at a shorter distance than electrostatic repulsions would impose without the covalent connection. As a result, the spontaneous curvature of the aggregates formed in aqueous solutions is lower than for their monomeric counterpart (i.e. the packing parameter is larger). Thus, wormlike micelles (WLM) form at very low concentration[8] without any salt or hydrophobic counterion as was not the case for the classically studied systems.[9] For $s = 6$–10, the distance between the positive charges becomes comparable to that of electrostatic equilibrium, the packing parameters are similar to that of the monomeric surfactants, and spherical micelles form up to high concentrations. For large values of s (≥ 14), the spacer loops within the aggregate like two additional hydrocarbon chains. These gemini surfactants

† Laboratoire de Dynamique des Fluides Complexes.
‡ Present address: IECB-Ecole Polytechnique, ENSCPB, Av. Pey Berland, BP 108 33402, Talence Cedex, France.
§ Laboratoire de Chimie Supramoléculaire.
‖ Institut de Génétique et de Biologie Moléculaire et Cellulaire.
⊥ Institut de Physique et Chimie des Matériaux de Strasbourg.
(1) Israelachvili, J. *Intermolecular & Surface Forces,* 2nd ed.; Academic Press: London, 1992; Part III.
(2) (a) Menger, F. M.; Littau, C. A. *J. Am. Chem. Soc.* **1991**, *113*, 1451. (b) Zana, R.; Benrraou, M.; Rueff, R. *Langmuir* **1991**, *7*, 1072.
(3) Danino, D.; Talmon, Y.; Zana, R. *Langmuir* **1995**, *11*, 1448.
(4) (a) Menger, F. M.; Littau, C. A. *J. Am. Chem. Soc.* **1993**, *115*, 10083. (b) Dreja, M.; Gramberg, S.; Tieke, B. *Chem. Commun.* **1998**, 1371. (c) De, S.; Aswel, V. K.; Goyal, P. S.; Bhattacharya, S. *J. Phys. Chem. B* **1998**, *102*, 6152.

(5) Sommerdijk, N. A. J. M.; Lambermon, M. H. L.; Feiters; M. C.; Nolte, R. J. M.; Zwanenburg, B. *Chem. Commun.* **1997**, 1423. Bhattacharya, S.; De, S. George, S. K. *Chem. Commun.* **1997**, 2287. Pestman, J. M.; Terpstra, K. R.; Stuart, M. C. A.; van Doren, H. A.; Brisson, A.; Kellog, R. M.; Engberts, J. B. F. N. *Langmuir* **1997**, *13*, 6857.
(6) Deinega, Y. F.; Ul'Berg, Z.; Marochko, L.; Rudi, V.; Denisenko, V. *Kolloidn. Zh.* **1974**, *36*, 649.
(7) (a) Oda, R.; Huc, I.; Candau, S. J. *Angew. Chem., Int. Ed. Engl.* **1998**, *37*, 2689. (b) Bhattacharya, S.; De., S. *Chem. Commun.* **1995**, 651.
(8) Kern, F.; Lequeux, F.; Zana, R.; Candau, S. J. *Langmuir* **1994**, *11*, 1714.
(9) Candau, S. J.; Hirtsche, E.; Zana R.; Adam, M. *J. Colloid Intface Sci.* **1988**, *122*, 430. Anet, F. A. L. *J. Am. Chem. Soc.* **1986**, *108*, 7102. Thurn, H.; Löbl M.; Hoffmann, H. *J. Phys. Chem.* **1985**, *89*, 517. Cates, M. E.; Candau, S. J. *J. Phys.: Condens. Matter* **1990**, *2*, 6869.

behave similarly to monomeric surfactants having two hydrocarbon chains (packing parameter between 0.5 and 1 and formation of vesicles).

Recently we reported on the synthesis of a series of dissymmetric gemini having the following structure and referred to as $n-2-m$:[10]
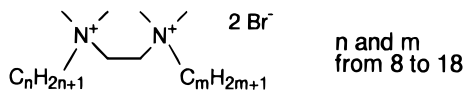
We characterized the phases formed by these surfactants in dilute ($\sim$1.0%) aqueous solutions and showed that decreasing the overall chain length ($n + m$) at a fixed chain length difference ($n - m$) or increasing chain length difference ($n - m$) at a fixed overall chain length both result in larger spontaneous curvatures. Thus, in the range of n and m studied, $8 \leqslant n, m \leqslant 18$ for small $n + m$ values or large $n - m$ (>2) values, only spherical or wormlike micelles (WLM) are formed, whereas for large $n + m$ values and small $n - m$ (<2) values, lamellar and tubular structures appear.

In the present study, we characterized the phases formed by these gemini surfactants at higher concentrations (15–95%) using rheology, X-ray scattering, and electron microscopy. We show that they assemble into a number of peculiar objects such as flat ribbons, stacks of ribbons, and elongated lamellar stacks. A strong tendency to form elongated and stacked structures emerges from these phase diagrams, which differ fundamentally from the phase diagrams of the corresponding monomeric ammonium bromides.[11]

Experimental Section

The studied surfactants $n-2-m$ were synthesized and recrystallized as described before.[10] The solutions were prepared using deionized water, and after thorough mixing at 65 °C, they were stored at 30 °C in an oven for 1 day to reach equilibrium.

Rheology measurements were carried out using a strain-controlled Rheometrics fluid spectrometer (RFSII) in cone–plate or Couette geometry. The cone–plate geometry consisted of a titanium upper cone of 25 mm diameter and an aluminum coated lower plate of 50 mm diameter; the Couette geometry consisted of a 34 mm diameter aluminum coated cup and a titanium bob of diameter 32 mm and height 33.3 mm.

It has to be remarked that some of the WLM solutions show a shear thickening phenomenon for a certain range of concentration around ϕ^* (e.g. the crossover concentration between a dilute regime of weak micellar growth and a semidilute regime of rapid micellar growth).[12] An increase in viscosity as well as a buildup of birefringence is observed at a certain shear rate. It has recently been proposed that this phenomenon is caused by a shear-induced phase separation between an aqueous phase poor in surfactant and either a locally surfactant rich phase with strongly branched and aggregated wormlike micelles[13] or a gellike structure.[14] The onset of this increase in viscosity can happen at a shear rate as low as 0.01 s^{-1} for certain systems, and once formed, this shear-induced structure can take as long as several thousand seconds to break down. This makes it very difficult to determine the zero-shear viscosity at around ϕ^*. In addition to this shear thickening effect in the vicinity of the crossover between dilute and semidilute regimes, many of the samples exhibit in the semidilute and concentrated regimes very long relaxation times, and the linear domain where the viscosity is independent of the shear rate exists only at very low shear frequencies such as 10^{-3} s^{-1} or below. Therefore, we had to make sure to apply low enough shear rates to avoid the above transition and perform measurements at equilibrium.

X-ray scattering measurements were performed using a linear monochromatic Cu Kα_1 beam obtained with a sealed tube generator and a bent quartz monochromator. Samples are sealed in glass capillaries of ca. 1 mm diameter and 10 μm thickness. The diffraction patterns were registered with a curved proportional detector "INEL CPS 120". Oriented patterns under a magnetic field of 1.2 T were obtained with a pinhole Cu Kα beam passing through a Ni-filter from a GX20 Eliot rotating anode X-ray generator. The samples are contained in the same glass capillaries as described above. The diffraction patterns were registered photographically.

Cryogenic Transmission Electron Microscopy of Vitrified Thin Film (Cryo-TEM of VTF) and Freeze Fracture. The samples were observed by transmission electron microscopy (TEM) after specific preparation. These techniques were used in order to obtain a direct imaging of the aggregates in solution. Which of these two techniques were used depended on the viscosity and concentration of the samples. Cryo-TEM of VTF has a high resolution but is not adapted to observe concentrated solutions (too much material in the thin frozen film in order to perform the transmission electron microscopy). So this technique was used for the samples with low viscoelasticity and low concentration <2%. On the other hand, freeze fracture is not adapted to observe objects such as small spherical or long micelles (diameter $\sim$40 Å). This technique was then used for the samples with higher viscosity and or concentration.

Cryo-TEM of VTF. Frozen-hydrated specimens were prepared as described.[13] The 700 mesh bare copper grids were dipped into surfactant solutions, the excess liquid was blotted with a piece of filter paper (Whatmann No. 2), and the grids were plunged into liquid ethane cooled with liquid nitrogen.[15] Grids were mounted under liquid nitrogen in a Gatan 626 cryoholder, transferred to the electron microscope, and observed at $\sim$−170 °C. Observations were made in a CM12 Philips microscope operating at 100 kV. The microscope was equipped with an additional anticontamination device.[16]

Freeze Fracture. Freeze fracture experiments were performed in an apparatus developed at IGBMC. Surfactant solutions were sandwiched between two copper specimen holders which were then frozen with liquid ethane cooled with liquid nitrogen. The frozen sandwich was then fixed to a transport unit under liquid nitrogen and transferred to the fracture replication stage, which was kept at a vacuum of 10^{-9} mbar at −180 °C, and then immediately after fracturing, replication took place by first shadowing with platinum/carbon at 45° and then deposition of carbon at 90°. The replica was then reinforced by collodion before the recuperation from the specimen holders. A drop of 1% solution of collodion in amyl acetate was deposited on the frozen surface of the replica while warming up to room temperature. The solvent then evaporates, leaving collodion to form a thin film over the replica. The replicas were then retrieved and cleaned in water; they were mounted on grids and soaked in methanol overnight to dissolve the collodion. Observations were made with a Zeiss EM 10CR microscope operated at 100 kV.

For both techniques, images were recorded on Kodak SO163 films and developed using standard procedures.

Results and Discussion

Solutions of several surfactants with various $n + m$ and $n - m$ values have been studied over a range of concentration ϕ (surfactant over water volume ratio) going from below their overlap concentrations ϕ^* (see Experimental Section) up to 95%. Rheological and optical (birefringence and texture) properties allowed us to define

(10) Oda, R.; Huc, I.; Candau, S. J. *Chem. Commun.* **1997**, 2105.

(11) Lequeux, F.; Candau, S. J. *Structure and Flow in Surfactant Solutions*; ACS Symposium Series No. 578; American Chemical Society: Washington, DC, 1994; Chapter 3, p 51.

(12) Ohlendorf, D.; Interthal, W.; Hoffmann, H. *Rheol. Acta* **1986**, *25*, 468.

(13) Oda, R.; Panizza, P.; Schmutz, M.; Lequeux, F. *Langmuir* **1997**, *13*, 6407.

(14) (a) Liu, C. H.; Pine D. J. *Phys. Rev. Lett.* **1996**, *77*, 2121. (b) Keller, S. L.; Pine, D. J.; Boltenhagen, P.; Zasadzinski J. A. *Phys. Rev. Lett.* **1998**, *80*, 2725.

(15) Adrian, M.; Dubochet, J.; Lepault, J.; McDowall, A. W. *Nature* **1984**, *308*, 32.

(16) Homo, J.-C.; Booy, F.; Labouesse, P.; Lepault, J.; Dubochet, J. *J. Microsc.* **1984**, *136*, 337.

(A)

(B)
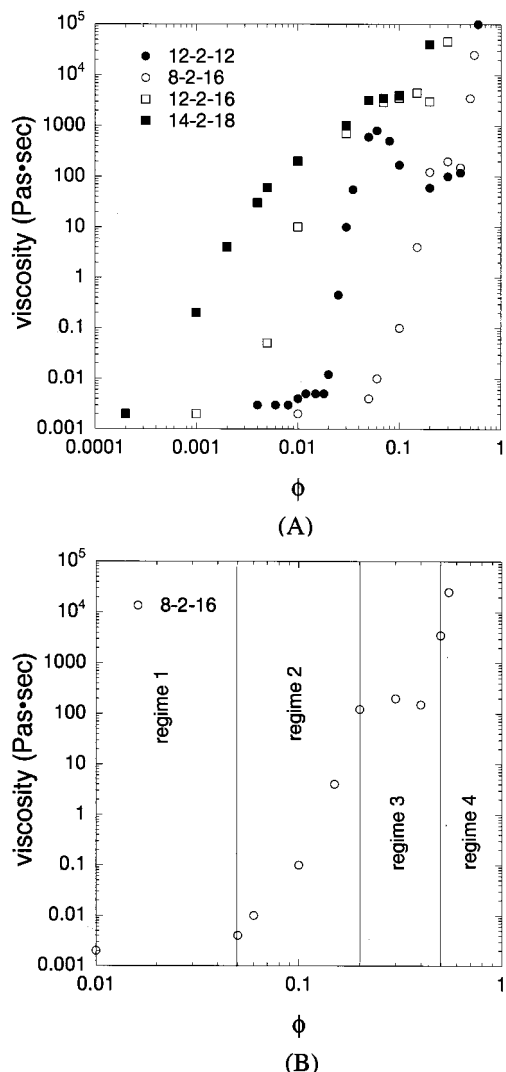
Figure 1. (A) Zero-shear viscosity (η) for surfactants $8-2-16$, $12-2-16$, $12-2-12$, and $14-2-18$, as a function of the concentration at 20 °C. (B) Various regimes of the viscosity behavior for $8-2-16$ surfactant.

several regimes (Figure 1). In the present study, we performed a structural investigation on two systems $8-2-16$ and $14-2-18$ with very different overlap concentration ϕ^*. These two systems follow a related but somehow different evolution as a function of concentration.

Regime 1. The solutions are transparent and isotropic with a viscosity about twice that of the water. This regime which extends from the CMC to ϕ^* has been observed in many salt-free systems and corresponds to dilute solutions of small spherical or ellipsoidal micelles.[17] The presence of such micelles can be assessed from cryo-TEM imaging. In this regime, the very strong electrostatic interactions prevent the micellar growth. At ϕ^*, the electrostatic interactions are screened out and the micellar growth becomes very rapid. The difference in the overlap concentrations of $8-2-16$ and $14-2-18$ surfactants can be explained from packing considerations: $8-2-16$ is very dissymmetric and has relatively short hydrophobic chain while $14-2-18$ is more symmetric and has longer hydrophobic chains. Therefore the end-cap energies, E_c, which are the energies to create two ends of micelles out of a cylinder, are very different for the two surfactants

(17) Safran, S.; Pincus, P.; Cates, M. E.; Mackintosh, F. C. *J. Phys. (Paris)* **1990**, *51*, 503.
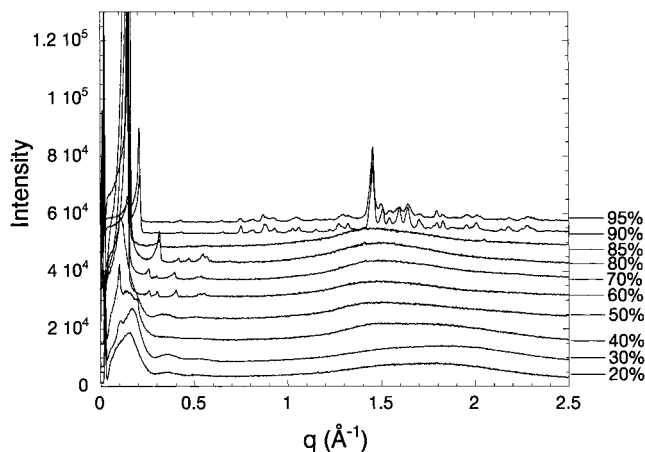
**Figure 2.** X-ray diffraction patterns of solutions of $8-2-16$ at various concentrations.

causing the difference in the overlap concentration, since $\phi^* \sim 1/E_c^2$ (see Appendix A).

Regime 2. The solutions are isotropic, transparent, and viscoelastic. The zero-shear viscosity increases rapidly with concentration. This regime extends from ϕ^* to a surfactant dependent concentration ϕ' at which the zero-shear viscosity levels off or decreases. For the $8-2-16$, ϕ' is ~20% whereas, for the $14-2-18$, ϕ' is not well defined but can be estimated to be about 2.5%, as confirmed by the appearance of birefringence in the solutions at rest beyond this concentration. The viscoelasticity of low concentration isotropic surfactant solution has been explained by the formation of entangled WLM. A coupled reaction—reptation model derived by M. Cates allows one to describe both linear and nonlinear viscoelastic behaviors of these systems.[18] One remarkable feature observed in many micellar systems is the quasi-Maxwellian behavior of the complex shear modulus. This occurs when the average micellar breaking time is much smaller than the reptation time of the micelles. For the gemini surfactant solutions studied here, the range of concentrations for which the solutions show a quasi-Maxwellian behavior varies depending on the surfactants: for $8-2-16$ solutions, we observed quasi-Maxwellian behavior up to about 10% before the deviation becomes evident. For the $14-2-18$ solutions, we observed a large departure from the Maxwellian behavior even at concentrations close to ϕ^*. Such a difference could be explained by much larger values of the breaking time for the $14-2-18$ solutions as it is known that breaking time of micelles is strongly system dependent. One can invoke another explanation based on the presence of objects other than WLM in the solution. This is confirmed by microscopic observation. For $8-2-16$ solutions, freeze fracture images (Figure 3a, b) show some stacked bilayer domains dispersed isotropically. The bilayer domain area is larger for the 20% solution. The periodicity of the bilayer can be roughly estimated to be ~40 Å, which corresponds to bilayers stuck to each other with almost no water between. These bilayer stacks are dispersed in aqueous domains where no structure is observed. These may contain spherical or wormlike micelles. For a solution of 20% which corresponds to the upper limit of regime 2, clear signals of a smectic-type order are seen up to the third-order peak, the first peak being at around 0.16 Å^{-1} in the X-ray spectrum (Figure 2). This indicates the presence a periodical arrangement of bilayer lamellae, and the periodicity agrees with the value measured from the freeze fracture images.

(18) Cates, M. E. *J. Phys. (Paris)* **1988**, *49*, 1593. Cates, M. E. *Macromolecules* **1987**, *20*, 2289.
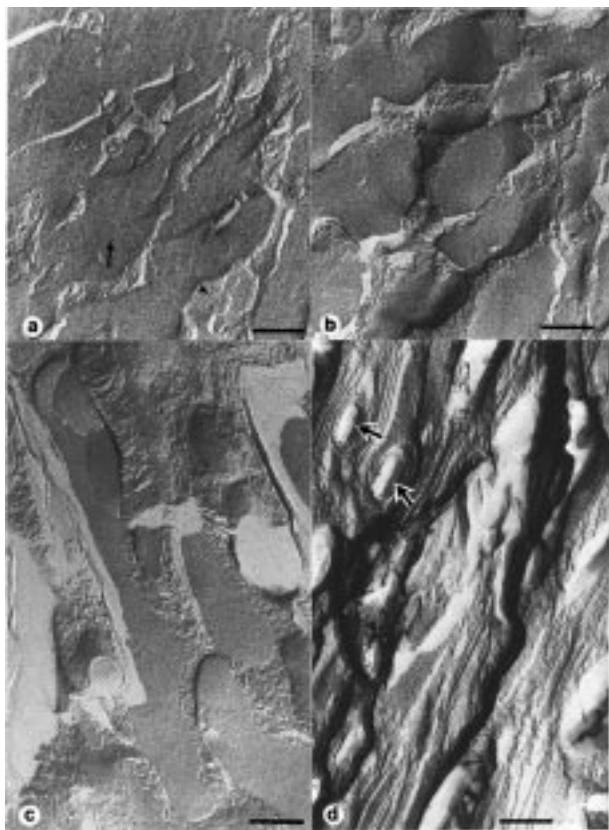
Figure 3. Freeze fracture images of $8-2-16$ solutions at different concentrations. (a) 15%: Arrowheads indicated the stacked bilayers which can clearly seen as stripes of dark and white layers. The domains are rather small and homogeneously dispersed in the bulk. The aqueous domains present a smooth surface (arrow). (b) 20%: The water domains are well defined and separated from each other by the surfactant domains. (c) 30%: The water domains and the layers are aligned in a direction. (d) 55%: The water domains are small, trapped in the aligned surfactant bilayers (arrows). Bar: 100 nm.

We also performed X-ray scattering measurements with a magnetic field of 1.2 T applied perpendicular to the incident X-ray beam. Below 20%, samples are not birefringent and the magnetic field has no effect: the scattered intensity remains isotropic confirming the absence of a correlation of layer normal orientation.

For $14-2-18$, regime 2 is attained at very low concentration which allowed us to perform cryo-TEM observations. The cryo-TEM images obtained in a 0.5% solution show that very long WLM coexist with a flat ribbonlike structure (Figure 4a) having the same width all along (width ~150 Å, length ~microns). The low electron density of these ribbons, as well as their thickness seen when they turn around themselves (normal of the ribbon surface in the plane of the observation), both indicate that they consist of a single bilayer. Sometimes, a WML can be seen changing into a ribbon along its length (Figure 4b).

Regime 3. The solutions are strongly birefringent, slightly translucent, and viscoelastic. For $8-2-16$ solutions, viscosity decreases upon increasing concentration in the range over $30-50\%$. Freeze fracture images at 30% show growth and directional alignment of the bilayer domains with a correlation length of a few microns (Figure 3c). As the concentration increases to 55%, the aqueous domains shrink (Figure 3d). From the freeze fracture images, it can be seen that the observed birefringence does not originate from the individual domains of bilayer stacks but from the long-range alignment of these domains. The appearance of the long-range correlation of the
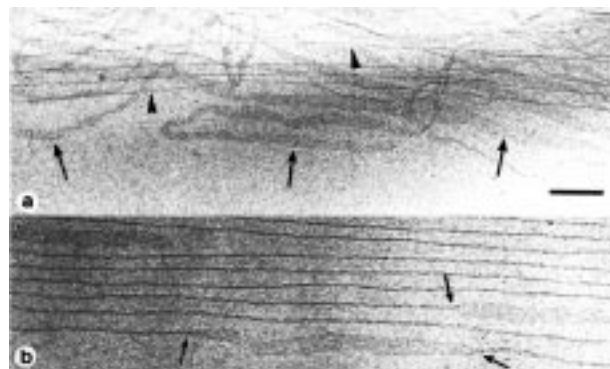
Figure 4. Cryo-TEM image of a vitrified thin film of $14-2-18$ surfactant 0.5% solution. Elongated micelles (a, arrowheads) coexist with elongated ribbons (a, big arrow). In (b) the transition between a WLM and a ribbon can be seen (arrows). Bar: 100 nm.

individual mean layer normal orientations as the concentration is increased from the isotropic (regime 2) and the expelled water volume is decreased corresponds to the transition from the isotropic phase to a phase which can be considered as nematic in nature.

The periodicity within the stacks measured by the X-ray scattering is still ~40 Å (Figure 2) which corresponds to the periodicity of the dry lamellae with no water between. Thus, this periodicity is independent of the concentration, which is unlike a typical lamellar phase whose periodicity follows a dilution law. This invariance of the peak position was also observed for the $10-2-16$ and $12-2-16$ solutions in this regime (data not shown).

Under a magnetic field, the diffused X-ray patterns become anisotropic. The intensity increases in the direction parallel to the field and decreases in the direction perpendicular to the field. This occurs without displacement of the peak position, indicating the existence of local lamellar ordering: the aggregates align along the magnetic field without any change in the periodicity, and that correlation between the aggregation is of short-range order. Between 30 and 50%, the smectic order coexists with another phase with its peak at about 0.1 Å^{-1}. The assignment of this peak to a hexagonal order is clearly validated at 60%, when the smectic order peaks disappear and the higher order peaks of the hexagonal phase appear.

For $14-2-18$, the solution is already birefringent at 3%. Freeze fracture images show that the ribbons observed in regime 2 are now stacked to form multilayered ribbons (Figure 5a,b). These ribbons are strongly interconnected. Their width is larger and less clearly defined than at 0.5%. The periodicity of the stacks calculated from the shadow of a bilayer step is also ~40 Å, similar to what was observed in $8-2-16$ systems. At higher concentrations (10 and 20%), the width of the ribbons increases further until it forms a three-dimensional network analogous to that observed for $8-2-16$, with a bilayer stack domain and an aqueous domain (Figure 5c,d).

Regime 4. This phase correspond to the emergence of a hexagonal order of packed long reversed micelles. The X-ray scattering spectra (Figure 2) show four to seven sharp reflections corresponding to the spacing ratios $1:\sqrt{3}:\sqrt{4}:\sqrt{7}:\sqrt{9}:\sqrt{12}:\sqrt{13}$ in the small-angle region. This type of pattern is typical of the hexagonal columnar phase. Within this phase, the aliphatic tails fill the space between the water columns surrounded by the polar heads and placed at the knots of a long-range correlated bidimensional hexagonal lattice. The transition from the lamellar to the columnar type of arrangement follows the cur-
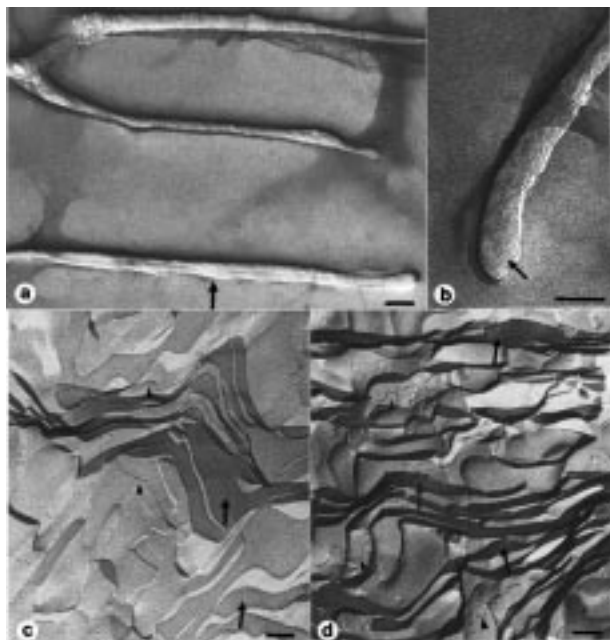
Figure 5. Freeze fracture images of 14−2−18 solutions at different concentrations: (a, b) 3%, long multilayered ribbons; (b) higher magnification, the multilayers can clearly be seen (arrows); (c) 10% stacks of bilayer (arrowheads) separated by large aqueous domains (arrows); (d) 20%, surfactant bilayer domains (arrowheads) are much larger than in (c) and the aqueous domain is reduced (arrows). Bar: 100 nm.
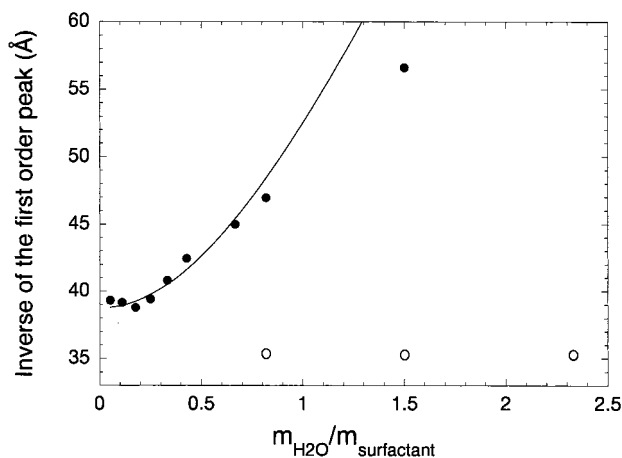
Figure 6. Peak position d as a function of water to surfactant weight ratio, fitted with the eq 1. The disagreement with the higher m_{H_2O}/m_{surf} is likely due to the coexistence with the collapsed lamellar phase.

vature of the aqueous paraffinic interface, related to the decrease of the amount of water included in the lamellar correlation domains. The first-order peak of this hexagonal phase marks the distance between water columns. Its position varies toward larger q values: the distance between the water column decreases with increasing surfactant concentration, as the concentration is increased up to 85% (8−2−16).

The position of the first-order peak corresponding to the hexagonal ordering is reported in Figure 6 as a function of water over surfactant weight ratio. By the assumption of a well-defined cylindrical interface between the water columns and the aliphatic filling, the number of surfactant molecules per unit length is linearly proportional to $n(r) \propto 2\pi r/S$, where S is the area per polar head, r is the radius of the water column, and the corresponding water volume is $v(r) \propto \pi r^2$. The volume ratio $\phi(r)$ is deduced:

$$\phi(r) = \frac{V_1 n(r)}{V(r)} = \frac{2\pi r V_1}{S \pi r^2} = \frac{2 V_1}{S} \frac{1}{r}$$

Here $MM_1/N\rho_{surf}$ is the molecular volume of the surfactant, MM_1 the molar mass, N, the Avogadro number, and ρ the density of the surfactant. The radius of the water columen is directly deduced from the columnar lattice area $2d^2/\sqrt{3}$ from the area of the virtual columnar lattice without the aqueous core $2d_0^2/\sqrt{3}$:

$$\frac{2d^2}{\sqrt{3}} = \frac{2d_0^2}{\sqrt{3}} + \pi r^2$$

and

$$r = \sqrt{\frac{2}{\pi\sqrt{3}}} \sqrt{d^2 - d_0^2}$$

From the relation between the water over surfactant mass ratio m_{water}/m_{surf} and the volume ratio $m_{water}/m_{surf} = (\rho_{water}/\rho_{surf})(1/\phi(r))$, where the ρ_{water} and ρ_{surf} are the densities of the water and of the surfactant, respectively, the following equation is deduced:

$$\frac{m_{water}}{m_{surf}} = \frac{1}{K}\sqrt{d^2 - d_0^2}$$

Thus,

$$d = \sqrt{K^2\left(\frac{m_{water}}{m_{surf}}\right)^2 + d_0^2} \qquad (1)$$

where the K is a factor considered to be constant, with the following expression:

$$\frac{1}{K} = \frac{\rho_{water}}{\rho_{surf}} \frac{S}{[2\pi(3^{1/2})]^{1/2} V_1}$$

Thus,

$$K = \sqrt{2\pi\sqrt{3}} \frac{MM_1}{N\rho_{water}} \frac{1}{S} \qquad (2)$$

The fit of the experimental variation of d using eq 1 gives (Figure 6):

$$d_0 = 38.7 \pm 0.4 \text{ Å} \qquad (3)$$

$$K = 35.4 \pm 0.6 \text{ Å}$$

The mean distance between the columns in a hexagonal arrangement without water can be calculated as $2d_0/\sqrt{3}$ (since d_0 is the inverse of the first-order peak at (1 0 0)). Using eq 3, it is 44.7 ± 0.4 Å, which is close to the bilayer thickness. It also confirms that the peak of the smectic order observed at concentrations between 20 and 50% originates from a tight stacking of bilayers, with very little water between. This implies that these phases consist of two domains: a concentrated domain where surfactants form collapsed bilayers and an aqueous domain. Upon increase of the concentration, the distances between these collapsed lamellae domains decrease but the peak position which reflects the periodicity within the stacks does not vary.

In this regime 4, where the hexagonal ordering is observed, the diffused pattern in the presence of a magnetic
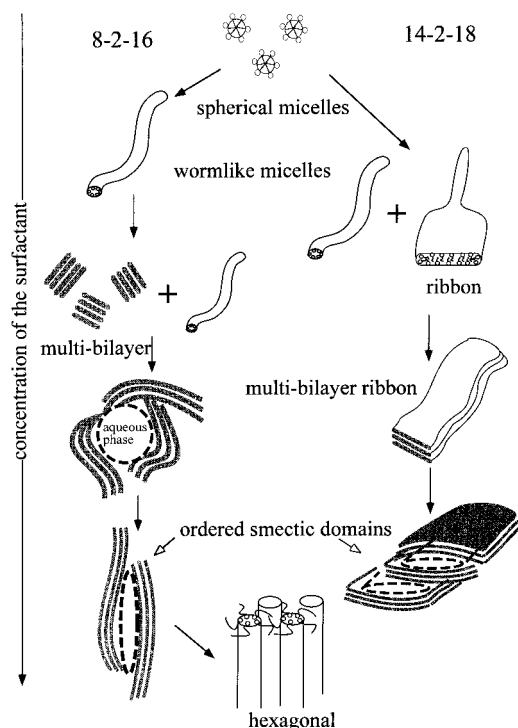
Figure 7. Schematic representation of the phases successively encountered as a function of the surfactant concentration.

field remains isotropic. This confirms the fact that the hexagonal order has a longer correlational length than the phases observed in regime 3. Thus it is much harder to align them with the magnetic field.

Above 90%, another transition is observed, toward a crystalline phase. At these concentrations, the broad peak at around 1.5 Å^{-1}, which is due to in-plane scattering by the surfactant molecules, sharpens into well-defined peaks (Figure 2). This shows that the hydrophobic chains undergo a transition from melt chain to crystallized chain.

Discussion

The phases formed by the cationic gemini surfactants studied here follow a series of changes as the concentration is increased. Starting from a dilute solution are successively encountered (1) spherical micelles, (2) a matrix of elongated micelles containing an increasing amount of bilayer structures which consist of long and thin ribbons or isotropically dispersed stacks of bilayers, (3) more or less connected ribbons or extended domains of stacked bilayers with orientational correlations, and (4) an inverted hexagonal columnar phase (Figure 7). Depending on the packing parameter of the gemini, these domains may cover a limited range of concentration (the ribbon domain, for instance, was not characterized for 8−2−16). The data presented here concern two representative *dissymmetric* gemini surfactants. Experiments performed on *symmetric* gemini surfactants establish that their behavior is essentially similar (see Figure 1A and ref 10). However, changing either the overall chain length ($n + m$) of the surfactant or its chain length difference ($n − m$) provides two means for tuning the packing parameter. This accurate control over the surfactant structure allows an easy access to the various phases encountered.

The succession of phases observed follows the classical decrease of spontaneous curvature as the concentration is increased. The appearance of elongated micelles at concentrations below 0.02% (ϕ^* for 14−2−18) shows that the decrease of spontaneous curvature occurs much more steeply for the dimeric surfactants. More importantly, this series is strikingly different and more complex than that observed for the monomeric surfactants or for dimeric surfactants with a longer flexible spacer ($6 \leq s \leq 10$).[19] Upon increasing concentration, trimethylalkylammonium bromides undergo changes from spherical micelles to elongated micelles (linear and possibly branched), nematic phases, hexagonal phases, and lamellar phases. In this case as well as for dimeric surfactants with a longer spacer, a normal (noninverted) hexagonal phase is observed between a micellar phase and a lamellar phase, which contrast with the inverted hexagonal phase reported here.

The succession of phases formed by 14−2−18 and 8−2−16 is also different from that of lipids and other surfactants with a single polar head and two hydrophobic chains such as didodecyldimethylammonium bromide (DDAB). For DDAB, Zemb et al. reported[20] that bilayers form at very low concentration ∼0.15%. Up to a certain concentration, (∼28% at 20 °C) the periodicity of the lamellar phase decreases as the surfactant concentration increases obeying the dilution law. Above this concentration, a coexistence of two lamellar phases, one swollen and the other collapsed, is observed for a large range of concentration. Above 75%, only the collapsed lamellar phase subsists, still following the dilution law.

Two remarkable features emerge from the series of phases reported here. The first one is an almost systematic tendency for these surfactants to form elongated aggregates: long micelles, ribbons.... In addition to the structures described here, this trend has been observed for a number of related surfactants that were shown to form tubules,[10] elongated vesicles,[21] or helical ribbons.[9a] This tendency cannot be accounted for on the sole basis of the packing parameter. A possible explanation is the existence of a nematic ordering of gemini molecules in the interface due to their elongated shape along the direction of the two charges. This would cause a difference in bending elasticities in directions parallel and perpendicular to the molecular orientation. We are presently investigating if such ordering exists in the plane of the interface.

The second remarkable feature is the strong attraction between bilayers of these surfactants, which are always observed in stacks. As seen from cryo fracture images and confirmed by X-ray scattering measurements, bilayers tend to stack and form multilayered structures with very little water in between. For $n−2−m$ gemini surfactant salt-free solutions, we never observe a normal lamellar phase following the dilution law. In the classical structure of a bilayer of charged surfactants, the resulting electrostatic term between stacked bilayers is repulsive. The collapse observed here can be attributed to the existence of an attractive force due to the interionic correlation resulting from the high affinity between the N$^+$ ions, separated by only 3 Å, and Br$^-$ ions. These Br$^-$ ions can serve as bridging between two positively charged interfaces. We have also observed strong attractive ionic forces between bilayers of gemini surfactant with a chiral counterion which forms hydrogen bonds.[9a] In that case, multilayered ribbons with very little water between twist into helical structures.

Conclusion

We have shown that, in water, cationic gemini surfactants of the series $n−2−m$ assemble in a rich variety of

(19) Alami, E.; Levy, H.; Zana, R. *Langmuir* **1993**, *9*, 940.
(20) Zemb, T.; Gazeau, D.; Dubois, M.; Gulik-Krzywichi, T. *Europhys. Lett.* **1993**, *21*, 759.
(21) Oda, R.; Bourdieu, L. Schmutz, M. *J. Phys. Chem. B* **1997**, *101*, 5913.

phases as concentration is increased. These phases are strikingly different from those observed for monomeric surfactants having one or two hydrocarbon chains and from other gemini surfactants with longer spacers ($n-s-n$ with $s > 4$). More specifically, preferences for elongated aggregates and stacked bilayers emerge as original features. The conjunction between the directional anisotropy of the gemini surfactants in the interface, due to their elongated shape along the direction of the two charges, and the strong ionic attraction between doubly charged headgroups and Br^- ions is likely at the origin of the observed phase behavior.

Appendix A: Rheological Behavior of WLM

The present study focused on the variation of viscosity of WLM solutions as a function of concentration. As was shown by MacKintosh et al.[17,22] wormlike micelles show an accelerated growth beyond ϕ^*, with a variation of the mean number N of subunits of the cylindrical micelles as a function of surfactant volume fraction ϕ, given by

$$N \propto 2\phi^{1/2} \exp[(E_c/2k_B T)\{1 - (\phi^*/\phi)^{1/2}\}] \quad \text{(I)}$$

where

$$\phi^* \approx (k_B T l_B \alpha v^{*2}/E_c)^2 \quad \text{(II)}$$

Here, E_c is the end-cap energy, the energy necessary to create two ends from a cylinder, v^*, the effective charge of micelles per unit length, l_B, the Bjerrum length, and α, the radius of the cylindrical micelles. For the series of gemini surfactants investigated here, the headgroups which carry the charges are unchanged from a surfactant to another one. Therefore, in eq II we can estimate that the only factor which affects the variation of ϕ^* is E_c; E_c increases as ϕ^* decreases, which is in agreement with the experimental observations. It was shown in our previous

study, that more symmetric surfactants molecules with longer hydrophobic chains are characterized by larger packing parameters which lead to lower ϕ^*.

Appendix B: Amount of Water in the Collapsed Lamellar Phase

By using K which was calculated in eq 2 and using $MM_1 = 614.68$ g/mol, $N = 6.023 \times 10^{23}$/mol, and $\rho_{water} = 0.99820 \times 10^{-24}$ g·Å^{-3}, the value of the area per polar head of the surfactant $8-2-16$ is deduced:

$$S = 95 \pm 3 \text{ Å}^2$$

This value largely exceeds the transverse area of a molten and stretched aliphatic chain (21.2 Å^2 at 20 °C for each chain[23]) indicating that the chains are strongly folded and/or interpenetrated. Consequently, by assuming the same value of S in the phases with local lamellar organization, the molten chains within the paraffinic bilayer could either be strongly folded or interpenetrated. Moreover, the thickness of the bilayer $d^{bilayer}$ is evaluated from S and from the surfactant density estimated to $\rho_{surf} = (0.90 \pm 0.04)10^{-24}$ g·Å^{-3} by using the partial volume additivity hypotheses and data over similar molecules:[24]

$$d^{bilayer} = \frac{2V_1}{S} = \frac{2MM_1}{N\rho_{surf}S} = 24 \pm 2$$

From $d^{bilayer}$ and from the aqueous sublayer thickness $d^{water} = d - d^{bilayer}$ ($d = 35 \pm 2$ Å, obtained from measurements), the water content within the lamellar correlation domains can be evaluated to

$$\frac{d^{bilayer}}{d^{water}} = 2.2 \pm 0.6$$

Thus, the collapsed lamellar phase includes about 30% water layer.

LA9814889

(22) Mackintosh, F. C.; Safran, S. A.; Pincus, P. A. *Europhys. Lett.* **1990**, *12*, 697.

(23) See for instance: Donnio, B.; Heinrich, B.; Gulik-Krzywichi, T.; Delacroix, H.; Guillon, D.; Bruce, D. W. *Chem. Mater.* **1997**, *9*, 2951. Seghrouchni, R.; Skoulios, A. *J. Phys. II* **1995**, *5*, 1547.
(24) Alami, E.; Levi, H.; Zana, R.; Neber, P.; Skoulios, A. *Liq. Cryst.* **1993**, *13*, 201.